Catena 272 (2026) 110383

Contents lists available at ScienceDirect

Catena

journal homepage: www.elsevier.com/locate/catena

Assessment of cropland carbon sequestration potential and its relationship with human activities: a case study in Jiangsu Province, China

Wenkai Cui [a], Jie Liu [a], Lei Zhang [b], Chenconghai Yang [a], Feixue Shen [c], Lin Yang [d,*]

[a] School of Geography and Ocean Science, Nanjing University, Nanjing 210023, China
[b] Climate and Ecosystem Sciences Division, Lawrence Berkeley National Laboratory, Berkeley, CA 94720, USA
[c] Xiangyang Institute of History and Culture & Hanjiang Institute, Hubei University of Arts and Science, Xiangyang 441053, China
[d] School of Public Administration and Policy, Renmin University of China, Beijing 100872, China

ARTICLE INFO

Dataset link: Reference data (Reference data)

Keywords:
Carbon sequestration potential
Cropland
Mineral-associated organic carbon (MAOC)
Human activities
Frontier line

ABSTRACT

Agricultural soils play a crucial role in the global carbon cycle, and the assessment of their carbon sequestration potential is essential for achieving carbon neutrality targets. While studies on the spatial distribution of carbon sequestration potential are emerging, limited research has focused on the linkage between carbon potential and human activities. This study focuses on assessing the carbon sequestration potential in a cropland of Jiangsu Province, China. Based on the mineral-associated organic carbon (MAOC) concentration of 84 surface soil samples, a frontier line method was employed to construct the curve of maximum MAOC concentration. A quantile random forest (QRF) model was employed to predict the spatial distribution of MAOC concentration across croplands. Then for each cropland grid, the maximum MAOC stock (MAOCS), the MAOCS deficit, and the carbon sequestration potential were calculated based on the predicted MAOC and the frontier line curve. Results indicate that northern regions of the Yangtze River (regions with intensive agricultural activities) tend to exhibit larger carbon deficit and higher carbon sequestration potential than southern regions of the Yangtze River (urban-dense regions). The correlation analysis of 11 human activity indicators shows that, indicators such as Main Crops (Grains) Sown Area and Total Power of Agricultural Machinery are negatively correlated with MAOCS, but positively correlated with both the MAOCS deficit and carbon sequestration potential. On the contrary, indicators such as Total Consumption of Electricity of the Year have an inverse relationship. This study provides a theoretical basis and practical reference for regional agricultural carbon management and sustainable agricultural development.

1. Introduction

Soil carbon is a key component of the global carbon cycle, accounting for over 60% of terrestrial carbon storage and playing a vital role in ecosystem function and climate regulation (Lal, 2004a). It accumulates through photosynthesis, microbial activity, and organic matter inputs, influencing energy flow and material cycling in ecosystems (Schlesinger and Andrews, 2000). Soil carbon sequestration potential refers to the soil's capacity to capture and stabilize atmospheric CO_2 under specific environmental and land use conditions, often measured by the amount and stability of soil organic carbon (SOC) (Batjes, 2014; Georgiou et al., 2022; Wiesmeier et al., 2014). This potential reflects both the soil's carbon sink capacity and its response to environmental and anthropogenic factors (Gregorich et al., 2009; Post et al., 2001; Wenzel et al., 2022). Regions with high carbon sequestration potential exhibit greater carbon accumulation rates, providing valuable insights for soil carbon storage strategies, also indicating greater carbon deficit and historical losses (Amelung et al., 2020; Bossio et al., 2020; Nolan et al., 2021). Soil carbon and its sequestration potential influence not only the soil's capacity to act as a carbon sink, but also the trajectory of climate change and the accuracy of long-term Earth system model projections (Georgiou et al., 2022). Thus understanding soil carbon potential is crucial for mitigating climate change, maintaining soil fertility, and enhancing ecosystem resilience (Arias et al., 2021), providing a scientific basis for optimizing land management and formulating climate adaptation strategies.

Agricultural ecosystems are among the most intensively human-managed systems globally, with agricultural land accounting for

* Corresponding author.
E-mail addresses: yanglin26@ruc.edu.cn, yanglin@nju.edu.cn (L. Yang).

https://doi.org/10.1016/j.catena.2026.110383
Received 22 May 2025; Received in revised form 27 June 2026; Accepted 29 June 2026
Available online 1 July 2026

approximately 38% of the Earth's terrestrial surface (Pu et al., 2024; Zomer et al., 2017). These systems are vital for ensuring food security and supporting economic development. Evaluating the carbon sequestration potential of soils is thus critical for agriculture, as it not only influences soil fertility and crop productivity but also directly contributes to climate change mitigation. Human activities in agricultural systems strongly influence SOC storage dynamics. For example, certain fertilizers enhance SOC content by supplying stable organic materials (Cotrufo, 2019). Conversely, the advancement of agricultural mechanization, while improving production efficiency, has also promoted practices such as deep tillage and frequent soil disturbance, which degrade soil structure and accelerate the oxidation and loss of particulate organic carbon (POC), leading to overall SOC decline (Breure et al., 2025). As De Rosa et al. (2024) observed, SOC content in European agricultural soils changed significantly between 2009 and 2018 due to management practices, with mechanized tillage particularly exacerbating carbon loss in cold and humid regions. In contrast, conservation practices such as reduced tillage or no-till farming can help preserve soil aggregates and enhance the stability of SOC (Stewart et al., 2007).

Various methods have been proposed in previous studies to estimate carbon sequestration potential. Hassink (1997) introduced the concept of "protection capacity" by establishing a linear relationship between the proportion of fine particles and organic carbon content, using the slope of the regression to represent the carbon concentration at the theoretical protective capacity (Six et al., 2002). While many studies have relied on SOC to calculate carbon sequestration potential (Chen et al., 2019; Wenzel et al., 2022), the growing focus on mineral-associated organic carbon (MAOC) has led to increasing interest in MAOC-based estimation methods (Six et al., 2024). MAOC, bound to fine particles via physico-chemical interactions, exhibits high stability and resistance to external disturbances such as tillage and climate change. Compared with POC, MAOC is less susceptible to loss and can be preserved long-term in agricultural soils (Cotrufo, 2019; Lavallee et al., 2020). According to Breure et al. (2025), MAOC is constrained by soil-climate conditions and reflects the upper limit of soil carbon storage according to its saturable nature. In summary, MAOC is not only a stable carbon pool but also a primary contributor to soil carbon accumulation in agricultural systems (Prairie et al., 2023), and is thus considered a key variable for evaluating carbon storage dynamics.

When calculating carbon sequestration potential via MAOC, the maximum MAOC stock (MAOCS) was used to represent the maximum theoretical carbon storage. The boundary line methods were commonly used to estimate maximum MAOCS (Feng et al., 2013; Beare et al., 2014; Georgiou et al., 2022). In the traditional boundary line method, the relationship of MOC (y-axis) was a function of clay and silt (x-axis), where the 95th quantile was a conservative approximation of the boundary line. While a limitation is that the upper boundary is determined manually using quantiles, which can result in some samples appearing above the theoretical maximum line. To overcome the limitation, Viscarra Rossel et al. (2024) used the frontier line method to estimate maximum MAOCS in Australia. This method is mathematically defined as a high conditional quantile function and approximates the upper envelope of the response variable distribution (Chen and Swanson, 2013). It captures the maximum achievable level under given environmental conditions, rather than the average trend, thereby providing a more reasonable representation of the upper limit, alleviating the impact of extreme values (McKenzie, 2018).

Although many studies have developed different methods for calculating sequestration potential and the focused on the impact of agricultural activities on soil carbon, few have directly explored the spatial relations between agricultural activities and carbon sequestration potential. Identifying which specific agricultural practices positively or negatively influence the potential can provide valuable insights for planning sustainable agricultural development and soil carbon conservation. To identify the potential correlation between agricultural activities and carbon sequestration potential, we selected Jiangsu Province as the study area because Jiangsu Province is one of China's major grain-producing regions. Since the 1980s, the trajectories of urbanization and agricultural modernization have varied significantly across different cities within the province (Yang et al., 2021; Zhang et al., 2026), likely resulting in spatial heterogeneity in soil organic carbon content and carbon sequestration potential.

Our study aims: (1) to calculate the theoretical maximum MAOC by frontier line method and quantify the MAOCS deficit and the corresponding carbon sequestration potential, (2) to assess relationship between carbon sequestration potential and agricultural human activities.

The innovation of this study is linking spatially human activity indicators to MAOC with quantile regression, thereby revealing how human activities drive carbon sequestration gaps in croplands.

2. Study area and dataset

2.1. Study area

Jiangsu Province is located in the central coastal region of China, in the lower reaches of the Yangtze River and Huaihe River, covering an area of 107,200 km^2. It is an important part of the Yangtze River Delta. The province spans from 30°45′ to 35°08′ N latitude and 116°21′ to 121°56′ E longitude. The plain area accounts for 86.90%, while the hilly area accounts for 11.54%, and mountainous area accounts for 1.56%. The plains of Jiangsu Province generally exhibit medium to high soil fertility and relatively flat terrain, which is favorable for large-scale mechanized agriculture. The province spans both the warm temperate and subtropical climate zones, with an annual average temperature ranging from 13 °C to 16 °C and annual rainfall between 800 and 1200 mm. In addition, the dense river network and numerous lakes provide favorable irrigation conditions that support crop water requirements and the cultivation of diverse agricultural crops. Jiangsu Province has favorable agricultural production conditions and is the largest japonica rice production province in southern China, as well as a key area for high-quality soft wheat production (https://www.zgjssw.gov.cn/shengqingbeilan/general/). In 2023, the total grain production of the province reached 37.977 million tons, an increase of 4.1 times over the past 75 years. The degree of agricultural mechanization in the province has continued to improve, further enhancing agricultural productivity (http://www.jiangsu.gov.cn/art/2024/10/4/art_88960_11377384.html). The study area and main water systems (the Yangtze River, Taihu Lake, Gaoyou Lake, Hongze Lake, and Luoma Lake) are shown in Fig. 1.

2.2. Dataset

2.2.1. Soil sample data

A total of 84 surface samples (0–20 cm) were collected from cropland areas within the study region, including the eastern plains, western mountainous areas, rural areas, and suburbs. The sampling was conducted throughout 2023, using a stainless-steel hand auger (inner diameter of 5 cm). Sample locations were determined by the conditioned Latin hypercube sampling method (Minasny and McBratney, 2006; Wang et al., 2024) and for each sample we used the five-point sampling method (Mao et al., 2020). Soil samples were collected separately, air-dried and passed through a 2 mm sieve and 150 mL 5‰ sodium hexametaphosphate (Marriott and Wander, 2006). The bottle filled with soils was then shaken for 18 h at 200 rpm to ensure thorough mixing. Subsequently, deionized water was continuously passed through a 53 μm sieve, ensuring the dispersion of the organic matter. All samples were dried at 50 °C and weighed, then sieved through 100 mesh (0.15 mm) prior to the measurement of MAOC concentration (g/kg) (See Table 1).

Based on the MAOC concentration, MAOCS (t/ha) were calculated using Eq. (1):

$$MAOCS = MAOC \cdot BD \cdot depth \cdot 0.1 \cdot (1 - frag) \tag{1}$$

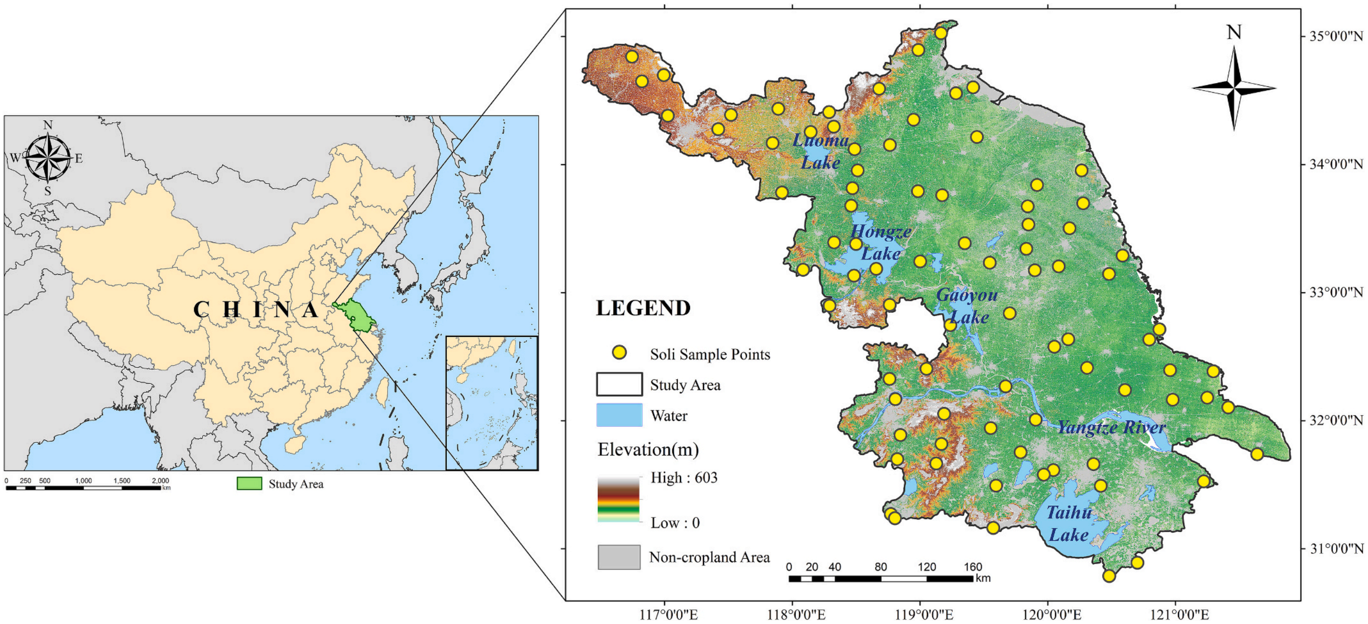

Fig. 1. Study area and the spatial distribution of samples.

Table 1
Statistical description of MAOC concentration (g/kg) based on the samples.

	Minimum	Maximum	Mean	Standard Deviation
Value	0.101	18.987	8.835	3.674

where *MAOC* is the MAOC concentration (g/kg), *BD* is the bulk density (g/cm^3), and *frag* is the coarse fragment proportion. Data on bulk density and coarse fragment proportion were obtained from Shi et al. (2025). Soil clay content and soil silt content data were also sourced from Shi et al. (2025). All the above datasets were resampled to a resolution of 90 m.

2.2.2. Environmental covariate data

In our study, the quantile random forest (QRF) method was used to predict the MAOC concentration in cropland grids. The original covariate set includes Digital Elevation Model (DEM), Topographic Wetness Index (TWI), slope, mean annual temperature (MAT), mean annual precipitation (MAP), mean annual evaporation (MAE), summer normalized difference vegetation index (NDVI), winter NDVI, soil sand content (sand), soil silt content (silt), soil clay content (clay), total nitrogen (TN), total potassium (TK), total phosphorus (TP), pH, cation exchange capacity (CEC), and soil organic carbon concentration (SOC). The DEM data were obtained from the Advanced Spaceborne Thermal Emission and Reflection Radiometer Global Digital Elevation Model (ASTER GDEM) with a resolution of 30 m. TWI and slope were calculated from the DEM data using ArcGIS, with a resolution of 30 m. Climate data, including mean annual temperature, precipitation, and evaporation (all at a 1 km resolution), were obtained from the National Tibetan Plateau / Third Pole Environment Data Center (Peng, 2022, 2020, 2019). NDVI data were retrieved from Sentinel-2 via Google Earth Engine and resampled to 90 m. The remaining soil property datasets were obtained from Shi et al. (2025), with a resolution of 90 m. DEM, TWI, slope and climate data were resampled to 90 m to ensure consistency in resolution. The resampling and data extraction of the grid layers were performed using the *terra* package in R.

2.2.3. Human activity data

Human activity data were obtained from the 2023 Statistical Yearbooks published by various cities in Jiangsu Province, which report statistics for the entire year of 2022. The used human activity indicators include Total Sown Area (1000 ha), Main Crops (Grains) Sown Area (1000 ha), Grain Production (10,000 t), Grain Yield per Unit Area (kg/ha), Consumption of Chemical Fertilizer (t), Total Power of Agricultural Machinery (10,000 kW), Total Consumption of Electricity of the Year (100 million kW·h), Total Consumption of Industrial Electricity of the Year (100 million kW·h), Employed Persons in the Primary Industry (10,000 persons), Employed Persons in the Secondary Industry (10,000 persons), and Employed Persons in the Tertiary Industry (10,000 persons),which were used to analyze the impact of human activities on the carbon sequestration potential of cropland.

2.2.4. Soil order, land use and administrative unit

Soil order classification data were acquired from the National Earth System Science Data Center (https://www.geodata.cn). According to the Second National Soil Survey of China (Office for the Second National Soil Survey of China, 1993), there are eight major soil orders in the study area: Luvisols, Saline Soils, Semi-luvisols, Dark Semi-hydromorphic Soils, Skeletol Primitive Soils, Ferralisols, Anthrosols, and Urban Lands. Other soil orders with small coverage are recorded as “Others” (Fig. 2a). As shown in the figure, in the northern and eastern regions of Jiangsu Province, Dark Semi-hydromorphic Soils are widely distributed, while in the central-western and southern regions, Anthrosols are more common. Saline Soils are distributed along the coastal areas in the eastern and northeastern parts. Luvisols are found in the northern and southwestern mountainous areas (elevation shown in Fig. 1), and are also distributed around Hongze Lake and Taihu Lake. Semi-Luvisols are found in the northwestern region, but cover a smaller area.

Land use data were obtained from Yang and Huang (2023) and were used to identify grids classified as cropland within the study region, with an original spatial resolution of 30 m, resampled to a resolution of 90 m. In terms of land use types (Fig. 2b), Jiangsu Province, as a typical agricultural province in China, has a widespread distribution of cropland, particularly in the northern and central regions where it dominates the landscape. In contrast, in the southern part of the province, especially along the Yangtze River, urban areas are dense and occupy a larger area (such as Changzhou City, Wuxi City, Suzhou City, Kunshan City, etc.), where Impervious land use is more common. Forest areas are located in the southwestern and central-western mountainous regions,

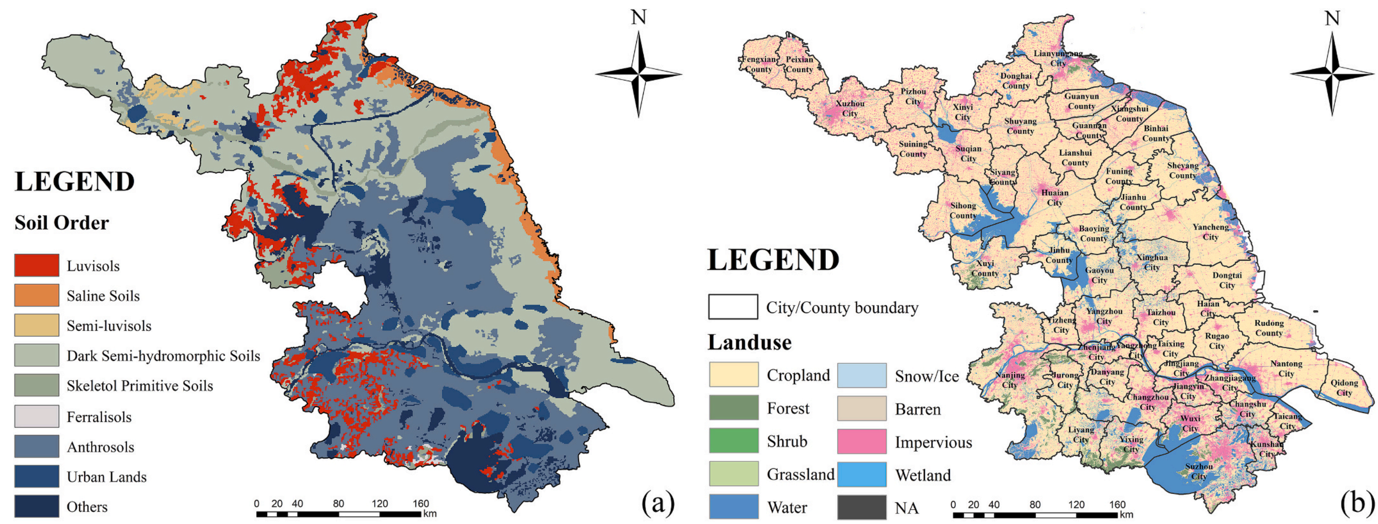

Fig. 2. Distribution of soil orders (a), administrative units and land use types (b) in Jiangsu Province.

but cover a smaller area.

Jiangsu Province contains 13 prefecture-level cities, which include 19 counties, 21 county-level cities and 55 districts in prefecture-level city in total. In this study, districts in prefecture-level cities were merged and referred to by the name of the corresponding prefecture-level city (e.g., Nanjing City), while counties (e.g., Suining County) and county-level cities (e.g., Jiangyin City) were treated as independent analysis units, resulting in a total of 53 administrative units (Fig. 2b).

3. Methodology

3.1. The overall framework of this study

Samples' MAOC concentration data was used to construct the maximum MAOC concentration curve by frontier line method, and predict all cropland grids' MAOC concentration with QRF. For each cropland grid, the MAOCS, the maximum MAOCS, the MAOCS deficit and the carbon sequestration potential were then calculated. The resulting grid data were subsequently classified by soil order and administrative units within Jiangsu Province to examine spatial distribution patterns and the relationships between carbon sequestration potential and human activities.

3.2. Construction of the maximum MAOC concentration frontier line

In this study, to ensure that the measured MAOC concentration remains below the theoretical maximum values, we used the frontier line method to represent the maximum achievable MAOC as proposed by Viscarra Rossel et al. (2024). Model was set up with 100 bootstrap trials, using concave fitting and 95% confidence interval, allowing the curve to envelop the entire set of samples and thus alleviating the issue of sample values appearing above the fitted line (Fig. 3). For all samples, a frontier line representing the maximum MAOC concentration was constructed using their observed MAOC concentration and corresponding clay + silt content. As the clay + silt content increases, the maximum MAOC gradually levels off. This aligns with the theory proposed by Hassink and Whitmore (1997), which suggests that as soil carbon nears its total capacity, the rate of further accumulation diminishes. The frontier line was constructed using the *snfa* package in R, based on the smooth non-parametric analysis method proposed by McKenzie (2018) with 100 bootstrap attempts (*method* = "mc").

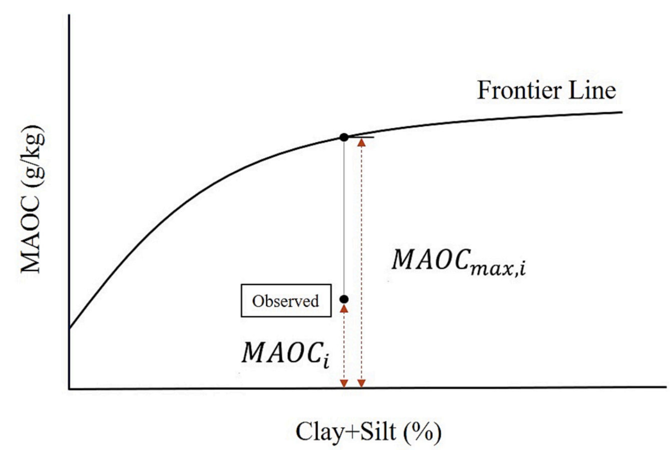

Fig. 3. The relationship between clay + silt content and maximum MAOC concentration represented by the frontier line (Georgiou et al., 2022; Viscarra Rossel et al., 2024). $MAOC_i$ is the observed MAOC concentration of sample *i*; $MAOC_{max,i}$ is the maximum MAOC concentration of sample *i*, calculated by the frontier line.

3.3. Prediction of cropland's MAOC for the study area based on machine learning

Random Forest (RF) is one of the most widely used machine learning (ML) algorithms in digital soil mapping (DSM) due to its ability to effectively capture nonlinear relationships, handle high-dimensional and multi-source data, and reduce the risk of overfitting through its ensemble learning framework (Bogaert et al., 2023; Khaledian and Miller, 2020). Conventional RF primarily provides estimates of the conditional mean response and does not directly quantify prediction uncertainty. To address this, Quantile Regression Forest (QRF), an extension of RF, enables the estimation of conditional quantiles and prediction intervals, thereby providing a practical framework for uncertainty quantification by retaining the full distribution of observations within terminal nodes (Nikou et al., 2022; Vaysse and Lagacherie, 2017). In this study, a QRF model was adopted to predict conditional mean MAOC concentration for cropland grids that derived based on land use. When predicting MAOC, Georgiou et al. (2022) used covariates including MAP, MAT, SOC, clay + silt, primary mineral type and land cover type, while Viscarra Rossel et al. (2024) incorporated multiple covariates spanning four domains: climate, vegetation, terrain, and mineralogy. In our study, the Recursive Feature Elimination (RFE) approach combined with cross-validation was employed to select an optimal combination of covariates with the *caret* package in R (Kuhn, 2008, 2007) from the original covariate set mentioned in Section 2.2.2.

A ten-fold cross-validation was performed using the existing samples, and the trained model was then used to predict MAOC concentration across all cropland grids. Grids missing any environmental covariate data are excluded and will not be calculated. In the model, the number of trees was set as 500, node size was 5, mtry was sqrt(p) where p is the number of covariates. We used R^2, root mean squared error (RMSE) and mean error (ME) to evaluate QRF model accuracy (mean value of ten-fold cross-validation). Eq. (2), (3) and (4) show how R^2, RMSE and ME are calculated in each fold.

$$R^2 = 1 - \frac{\sum_{i=1}^{n}\left(y_{pre,i} - y_{obs,i}\right)^2}{\sum_{i=1}^{n}\left(y_{pre,i} - \overline{y_{obs}}\right)^2} \tag{2}$$

$$RMSE = \frac{1}{\sqrt{n}}\sqrt{\sum\nolimits_{i=1}^{n}\left(y_{pre,i} - y_{obs,i}\right)^2} \tag{3}$$

$$ME = \frac{1}{n}\sum_{i=1}^{n} y_{pre,i} - y_{obs,i} \tag{4}$$

where n is the total number of validation samples; $y_{pre,i}$ is the predicted value for the i-th validation sample; $y_{obs,i}$ is the observed value for the i-th validation sample; $\overline{y_{obs}}$ is the mean of the observed values for the validation sample set.

In addition, we used 90% interval width to assess the uncertainty of the QRF model predictions. The QRF model was implemented using the *quantregForest* package in R.

3.4. Calculation of cropland's MAOCS deficit and carbon sequestration potential

For each cropland grid, the value of clay + silt was input into this frontier line to derive the corresponding maximum MAOC concentration. Both the predicted MAOC concentration and the estimated maximum MAOC concentration were then used to calculate MAOCS and maximum MAOCS as mentioned by Eq. (1). Subsequently, for each cropland grid, the MAOCS deficit was obtained using Eq. (5):

$$MAOCS_{def,i} = MAOCS_{max,i} - MAOCS_i \tag{5}$$

where $MAOCS_{def,i}$ is the MAOCS deficit of grid i; $MAOCS_{max,i}$ is the maximum MAOCS of grid i estimated using the frontier line; and $MAOCS_i$ is the MAOCS value of grid i. After obtaining the MAOCS deficit for each cropland grid, the carbon sequestration potential of grid i ($Carbon_{pot,i}$) is calculated using Eq. (6):

$$Carbon_{pot,i} = \frac{MAOCS_{def,i}}{MAOCS_{max,i}} \times 100\% \tag{6}$$

3.5. Statistical analysis based on soil order and administrative unit with human activity

In this study, two types of statistical analyses were conducted on cropland's MAOCS, maximum MAOCS, MAOCS deficit, and carbon sequestration potential. The first analysis involved examining these across different soil orders. Cropland grids were classified based on the spatial distribution of each soil order, which means analysis was performed on the grids that fell within each soil order. MAOCS, maximum MAOCS, MAOCS deficit, and carbon sequestration potential was visualized using quartile-based statistics using Eq. (7) and (8).

$$Q_k^j\left(Unit_p\right) = \text{Quantile}_k\left(\left\{Value_i^j | g_i \in Unit_p\right\}\right), k \in \{0.25, 0.5, 0.75\} \tag{7}$$

$$D_p^j = \left\{x \middle| x \in \left[Q_{0.25}^j\left(Unit_p\right), Q_{0.75}^j\left(Unit_p\right)\right]\right\} \tag{8}$$

Where $Unit_p$ is the soil order p; $Q_k^j(Unit_p)$ is the k-th quantile for the calculated content j (including MAOCS, maximum MAOCS, MAOCS deficit, and carbon sequestration potential) in the soil order p; g_i is i-th grid located in soil order p; $Value_i^j$ is the i-th grid's value for content j; D_p^j is the distribution of content j of soil order p.

The second analysis investigated the correlation between human activities and MAOCS, maximum MAOCS, MAOCS deficit, and carbon sequestration potential across different administrative units. After classified grids with MAOCS, maximum MAOCS, MAOCS deficit, and carbon sequestration potential into each administrative unit (the same as calculated for each soil order using Eq. (7) and (8), where $Unit_p$ is administrative unit p here) respectively, correlations between the human activity indicators and the median values of MAOCS, maximum MAOCS, MAOCS deficit, and carbon sequestration potential ($Q_{0.5}^j$) were calculated, and regression lines were fitted accordingly using Eq. (9).

$$y_{p,j}^q = \beta_{p,j}^q \cdot Q_{0.5}^j\left(Unit_p\right) + \alpha_{p,j}^q \tag{9}$$

where $y_{p,j}^q$ is the regression line between the human activity indicator q and the calculated content j of the administrative unit p; $\beta_{p,j}^q$ and $\alpha_{p,j}^q$ are the regression coefficient in the corresponding regression line.

4. Results

4.1. Fitted frontier line based on observed samples

The frontier line derived from the observed samples is shown in Fig. 4. During the construction of the frontier line, non-parametric bootstrap resampling for 100 times were conducted on the existing sample set to estimate the 95% confidence interval, which is also displayed.

4.2. Predicted MAOC concentration and uncertainty of Jiangsu cropland

With the *caret* package, finally selected covariates included two

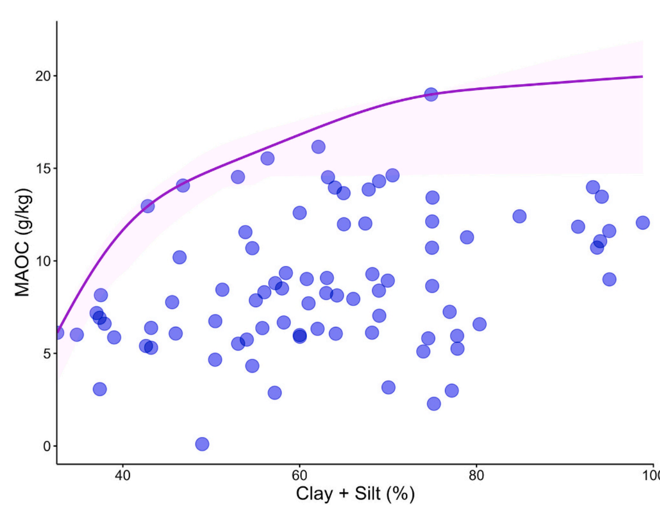

Fig. 4. The frontier line based on observed samples and the 95% confidence interval. Blue dots represent the soil samples, the purple line represents the fitted frontier line, and the purple shaded area represents the 95% confidence interval. (For interpretation of the references to colour in this figure legend, the reader is referred to the web version of this article.)

topographic covariates (DEM, TWI), three climatic covariates (MAT, MAP, MAE), two vegetation covariates (summer NDVI, winter NDVI) and four soil property covariates (sand, silt, TN, SOC), 11 in total. The QRF model was trained with the selected environmental covariates using the MAOC concentration of 84 samples as training data. The model's average accuracy based on a ten-fold cross validation was shown in Table 2.

Applying this model, MAOC concentration for all cropland grids were predicted, and the results are shown in Fig. 5(a). The prediction uncertainty results are shown in Fig. 5(b), where higher values indicate that the corresponding area may have sparse data or weak relationships between environmental covariates and the target variable, implying higher uncertainty.

In Fig. 5(a), the MAOC concentration in the northern part of Jiangsu Province is relatively low, while the central region has higher values, with higher MAOC concentration around water systems compared to other areas. In the northern and central parts of Jiangsu Province, the MAOC concentration is lower near urban areas (the gray radial regions in the figure), while rural areas farther from cities show significantly higher MAOC concentration. This is particularly noticeable in the densely urbanized areas to the south of the Yangtze River. In Fig. 5(b), the uncertainty in the eastern coastal areas and areas around the Hongze Lake is higher. In contrast, the uncertainty is lower in the northwestern areas and densely urbanized areas south of the Yangtze River.

4.3. Maximum MAOCS, MAOCS deficit, and carbon sequestration potential of cropland grids

According to the method described in Section 3, the cropland grids' MAOCS (Fig. 6a), maximum MAOCS (Fig. 6b), MAOCS deficit (Fig. 6c), and carbon sequestration potential (Fig. 6d) were then obtained respectively. Non-cropland areas, including urban regions, water bodies, and mountainous areas, are displayed separately in these figures.

After converting the predicted MAOC concentration to MAOCS, it was found that the MAOCS were relatively low in the northern and eastern coastal regions of Jiangsu Province. In contrast, the inland areas in the northwest exhibited slightly higher MAOCS than those in the east. Notably, the urban-dense regions in the south, areas surrounding Taihu Lake, and the Yangtze River showed significantly higher MAOCS than other parts of the study area. For the maximum MAOCS, the highest values were observed in the western part of Jiangsu Province, particularly around Nanjing City and the areas surrounding Hongze Lake. Additionally, high maximum MAOCS values were also found in the northern parts of Dongtai City, Hai'an City, Rudong County, and Nantong City. The MAOCS deficit and carbon sequestration potential showed similarly high values around Nanjing City and Hongze Lake, as well as in the central region of Jiangsu Province and the eastern areas north of the Yangtze River. In Qidong City, which is surrounded by the Yangtze River estuary and the sea, both the MAOCS deficit and carbon sequestration potential were higher than those in Nantong City—opposite to the spatial pattern of maximum MAOCS. However, in the urban-dense regions south of the Yangtze River—such as Changzhou City, Wuxi City, and Suzhou City—both the MAOCS deficit and carbon sequestration potential were significantly lower.

4.4. Statistical analyses by soil orders and administrative units

After classifying the MAOCS, maximum MAOCS, MAOCS deficit, and carbon sequestration potential by soil orders, the statistical results were presented in the form of quartiles, as shown in Fig. 7. For the predicted MAOCS, the median values for Luvisols, Saline Soils, Skeletol Primitive Soils, and Dark Semi-hydromorphic Soils are relatively low—approximately 32.0 t/ha—with narrow interquartile ranges, indicating compact distributions. Semi-Luvisols also show a compact distribution but with a higher median compared to the aforementioned soil orders. Anthrosols and Urban Lands have slightly higher medians and somewhat wider interquartile ranges, suggesting greater variability. In contrast, for the maximum MAOCS, the medians of most soil orders fall within the range of 68–70 t/ha. Luvisols, Saline Soils, Skeletol Primitive Soils, and Dark Semi-hydromorphic Soils exhibit relatively high values, which markedly differ from their predicted MAOCS distributions. Among them, Skeletol Primitive Soils have the highest median, while Luvisols show the widest interquartile range, indicating the greatest variability. The distributions of MAOCS deficit and carbon sequestration potential are similar. Luvisols, Saline Soils, Skeletol Primitive Soils, and Dark Semi-hydromorphic Soils show higher median values, whereas Anthrosols, Urban Lands, Semi-Luvisols, and Ferralsols have lower distributions. The large variability in the maximum MAOCS for Luvisols contributes to their greater variability in MAOCS deficit as well.

After categorized by administrative units, quantiles were calculated for each category, and integrated rankings were performed based on different human activity indicators. The calculated coefficient of determination (R^2), significance probability (*p*-value), and correlation coefficient (r) were shown in Fig. 8. Given the high similarity in results of the above statistical indicators between the MAOCS deficit and carbon sequestration potential and the significance level of maximum MAOCS is poor (all 11 selected human activity indicators demonstrated weak linear relationships, with R^2 values below 0.1, p values greater than 0.1, and absolute r values around 0.1), this study presented only the results of MAOCS and carbon sequestration potential in the Fig. 8 for clarity and conciseness.

For MAOCS, indicators such as Main Crops (Grains) Sown Area, Grain Production, Consumption of Chemical Fertilizer, and Employed Persons for Primary Industry showed relatively strong negative correlations, all with p values less than 0.01. Among them, Main Crops (Grains) Sown Area and Grain Production exhibited R^2 values around 0.4, indicating significant negative relationships with MAOCS. In contrast, Total Consumption of Electricity of the Year, Total Consumption of Industrial Electricity of the Year, and Employed Persons for Secondary Industry showed relatively strong positive correlations, with r values exceeding 0.5 and p values below 0.01. As for carbon sequestration potential, indicators such as Main Crops (Grains) Sown Area and Grain Production showed relatively strong positive correlations. Conversely, Total Consumption of Electricity of the Year and Total Consumption of Industrial Electricity of the Year demonstrated relatively strong negative correlations.

In Fig. 8, each subgraph represents the quantile regression result of one human activity indicator with MAOCS or carbon sequestration potential. In each subgraph, the dashed line represents the fitted regression line, each gray dot represents an administrative unit's median (Q2) value, while the upper and lower whiskers represent the third (Q3) and first (Q1) quartiles, respectively.

5. Discussion

5.1. Carbon sequestration potential of different soil types

Our study found that carbon sequestration potential exhibited distinct distribution patterns across different soil orders, which might be attributed to their inherent pedogenic processes as well as varying degrees of anthropogenic influence. The northern and eastern regions of Jiangsu Province are dominated by large areas of Dark Semi-hydromorphic Soils. These soils have formed under the combined influence of intermittent water saturation, low-lying topography, partial clay formation from sandy parent materials, and vegetation succession,

Table 2
Accuracy evaluation results.

Index	R^2	RMSE	ME
Value	0.75	2.19	0.05

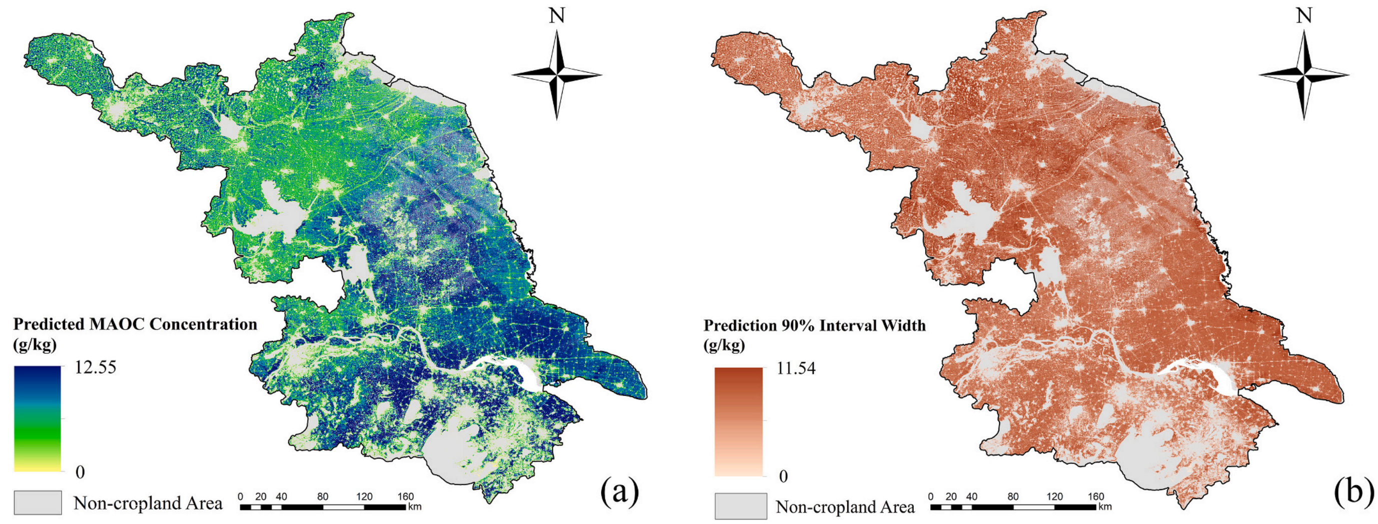

Fig. 5. Predicted MAOC concentration (a) and the prediction 90% interval width of quantile random forest model (b) for cropland grids.

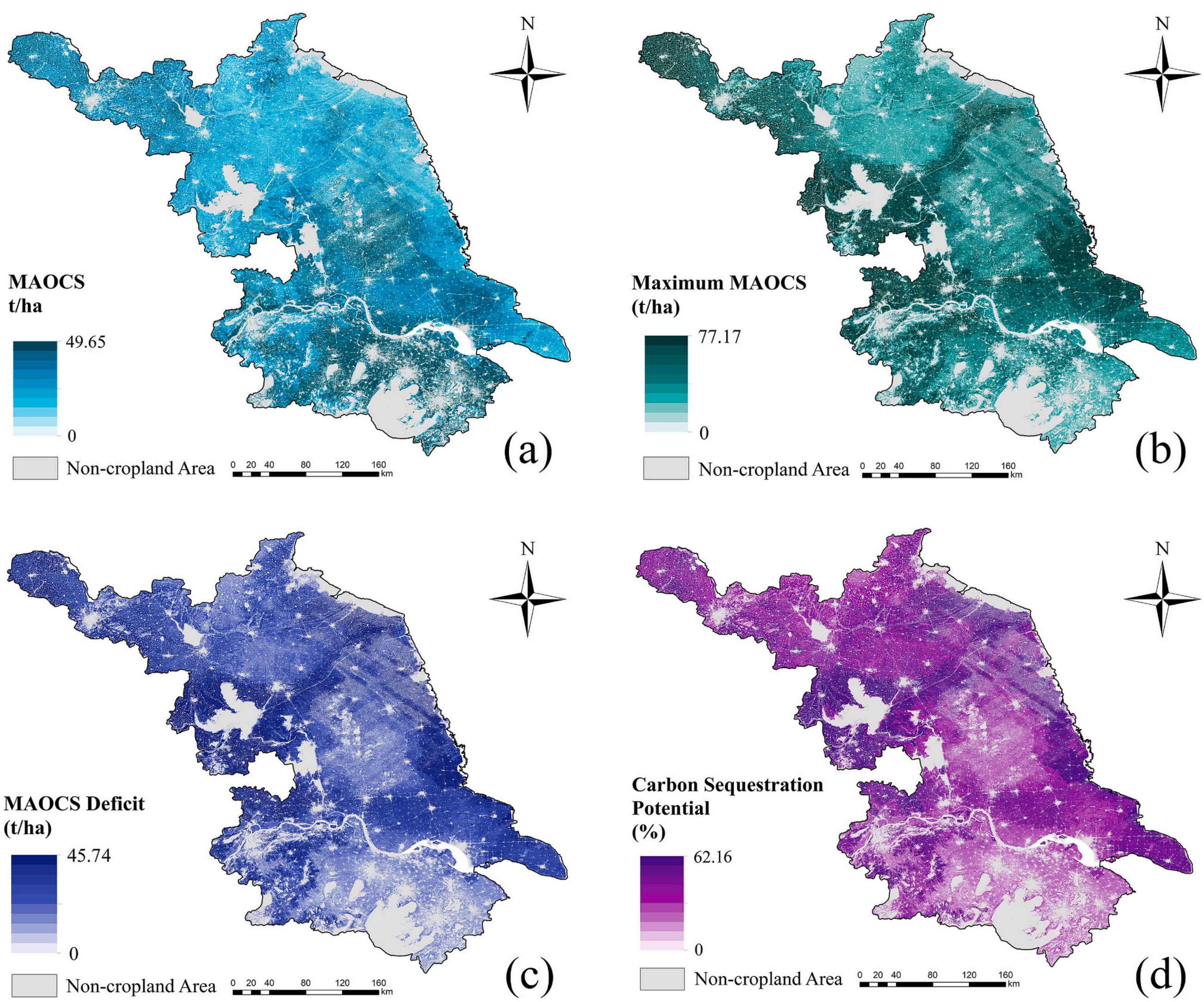

Fig. 6. Cropland grids' MAOCS (a), maximum MAOCS (b), MAOCS deficit (c), and carbon sequestration potential (d).

making their carbon sequestration potential closely related to local moisture regimes and vegetation development (Likhanova et al., 2022). Once water availability becomes limiting, the rate of organic carbon storage declines (Likhanova et al., 2022; Xu et al., 2019), resulting in a

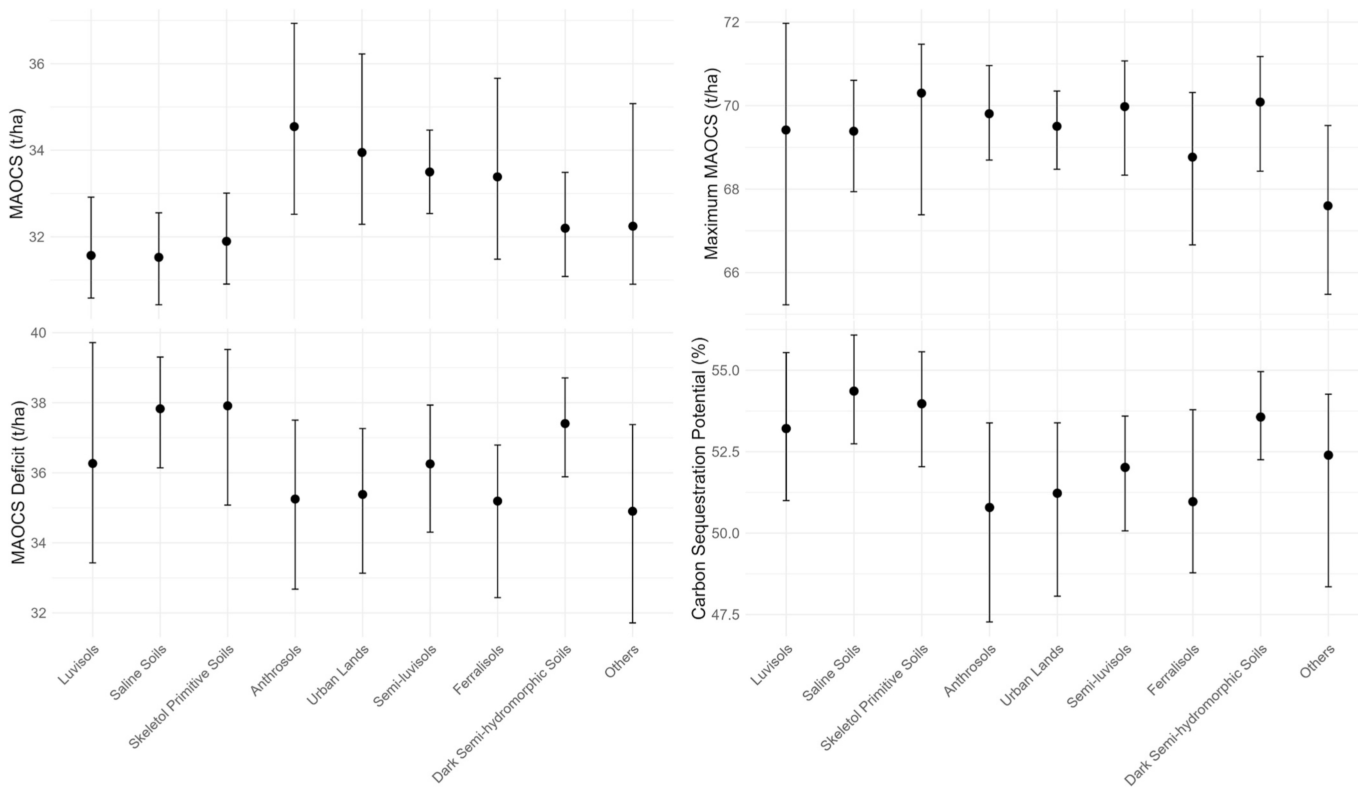

Fig. 7. The MAOCS, maximum MAOCS, MAOCS deficit, and carbon sequestration potential for each soil order category. The upper and lower whiskers represent the third quartile (Q3) and the first quartile (Q1), respectively, while the black dots indicate the median (Q2).

less stable carbon storage capacity than that of Anthrosols. Consequently, Dark Semi-hydromorphic Soils exhibit lower MAOCS, but higher MAOCS deficit and carbon sequestration potential.

In southern Jiangsu Province, where most major cities are located, Anthrosols predominate in cropland areas. Anthrosols are soils that have been altered due to human activities, with agricultural practices being the most dominant cause of their formation (Holliday, 2022). Persistent tillage and irrigation have altered soil physicochemical properties, such as pH and clay content, thereby affecting the adsorption capacity of minerals for organic carbon and promoting the accumulation of MAOC (Cotrufo, 2019). In addition, long-term fertilization has been shown to enhance the activity of certain microbial communities (Woolf and Lehmann, 2019). The metabolic by-products and microbial residues generated in these systems have also contributed to the accumulation of MAOC. Anthrosols currently exhibit relatively high MAOCS levels, which, in turn, results in lower MAOCS deficit and carbon sequestration potential. Detailed human activities in agriculture will be further discussed in Section 5.2.

For Luvisols, the topsoil has undergone long-term leaching, leading to the loss of organic matter and nutrients through water runoff, which results in relatively low organic carbon accumulation (Pikuła et al., 2025). Additionally in Jiangsu Province, Luvisols are mainly distributed in mountainous areas and surrounding regions, where the topographical relief further complicates the accumulation of organic carbon.

For Saline Soils, particularly those located along the coast, the high salinity and alkalinity negatively affect plant health, reducing the amount of organic carbon transferred into the soil and lowering the organic carbon pool content (Wong et al., 2010). Moreover, excess salt inhibits microbial biomass (Ghollarata and Raiesi, 2007; Wichern et al., 2006), the mineralization of carbon and nitrogen, and soil enzyme activity (Pathak and Rao, 1998; Tripathi et al., 2007), further impacting the organic carbon storage in the soil (Dendooven et al., 2010). In the eastern and northeastern parts of Jiangsu Province, Saline Soils have been partially reclaimed for agricultural use. However, due to the high salinity and alkalinity of the soil, the MAOCS are relatively low, while the MAOCS deficit and carbon sequestration potential are high.

5.2. The impact of human activities to cropland's soil carbon sequestration potential

In agricultural ecosystems, agricultural development through activities such as tillage, planting, fertilization, and irrigation directly or indirectly affects the input, decomposition, and storage of SOC. Therefore, the assessment of carbon sequestration potential may provide a useful reference for evaluating agricultural management practices and offer insights for policy adjustments aimed at enhancing the sustainability of both agriculture and soil systems. Key management practices such as tillage, fertilization, and crop rotation may influence MAOC dynamics by altering soil structure, microbial activity, and the balance between carbon inputs and outputs, thereby potentially influencing both SOC storage and carbon sequestration potential (Lal, 2004b; Ludwig et al., 2011; Meng et al., 2024). Previous studies have reported that China's cropland carbon stocks increased from the 1980s to the 2000s under land management practices such as the incorporation of crop residues and organic manure, increased application of synthetic fertilizers with optimized nutrient combinations, and the adoption of no-tillage methods. However, substantial carbon sequestration potential still remains (Lu, 2015; Song et al., 2014; Tao et al., 2019). The Yangtze River region in China has a long history of agricultural development and other anthropogenic activities, which have intensified significantly since the 1950s (Cui et al., 2022; Yin et al., 2022). By the year 2000, more than 10,000 km^2 of land had been reclaimed for agriculture over the previous five decades (Du et al., 2011). These human activities are widely considered to be closely linked with changes in local soil morphology. For example, some practices in land development and farmland reclamation have been reported to be associated with organic carbon loss from cropland soils at different rates, resulting in relatively low organic carbon content in agricultural soils (Lal, 2004b; Poeplau

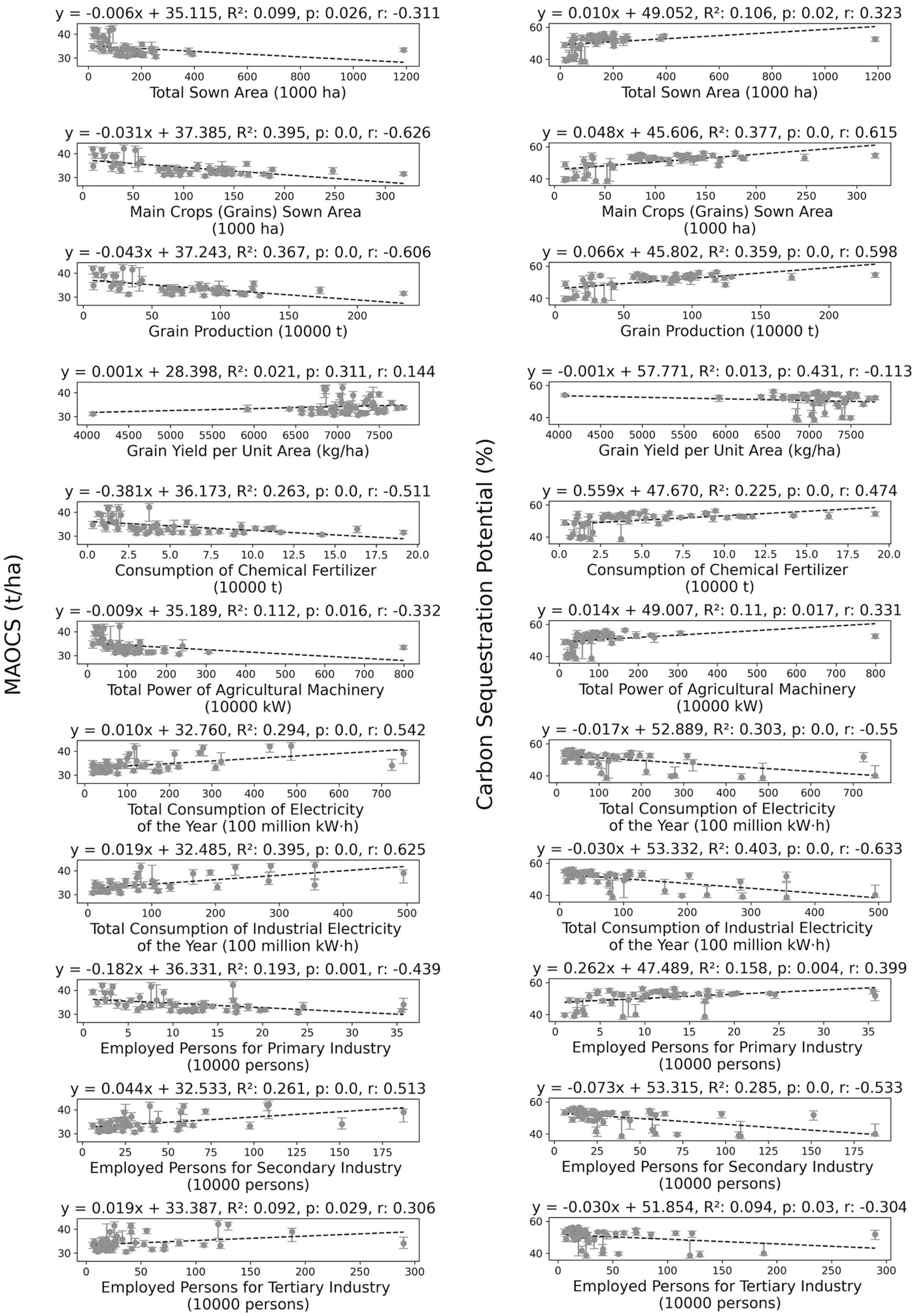

Fig. 8. The distributions of MAOCS and carbon sequestration potential across different administrative units, categorized based on various human activity indicators.

and Don, 2015).

Both the Main Crops (Grains) Sown Area and Grain Production exhibit a strong negative correlation with MAOCS in our results, suggesting that regions with larger areas of grain crop cultivation may be associated with lower levels of SOC. For instance, Huaian City has the largest values for both Main Crops (Grains) Sown Area (318,200 ha) and Grain Production (2,337,500 t). At the same time, its Total Sown Area is 392,360 ha, suggesting a high proportion of grain crops, and its MAOCS is lower than those of other administrative units. Correspondingly, administrative units with lower MAOC levels tend to exhibit higher carbon sequestration potential. One possible explanation is that intensive crop cultivation may be linked to greater depletion of soil carbon, thereby creating a larger gap from the theoretical maximum carbon storage and, consequently, a higher theoretical carbon sequestration potential. However, it should be noted that a larger carbon deficit does not necessarily indicatea higher feasible sequestration potential, as actual carbon accumulation is constrained by factors such as soil properties, climate conditions, and management practices. This association may be partly explained by several underlying mechanisms, including enhanced soil disturbance from frequent tillage, increased biomass removal during harvest, and reduced return of organic residues to the soil.

In addition, Total Power of Agricultural Machinery shows a moderate negative correlation with MAOCS, and a slightly positive correlation with carbon sequestration potential. As an indicator of the level of agricultural mechanization, the increase in Total Power of Agricultural Machinery promotes the development of agricultural mechanization and realizing agricultural modernization to some extent (Ju et al., 2016; Meng et al., 2024), reflecting the degree of agricultural exploitation in each administrative unit. Similar to Main Crops (Grains) Sown Area and Grain Production, higher values are associated with lower MAOCS and higher carbon sequestration potential. This pattern may suggest that regions with more intensive cultivation are associated with greater soil carbon loss related to crop growth and harvesting processes, thereby exhibiting larger carbon deficits and higher carbon sequestration potential. In addition, higher levels of mechanization may be associated with more intensive land use practices, such as deeper or more frequent tillage and shorter fallow periods (Ju et al., 2016; Kim et al., 2025), which could accelerate soil organic matter decomposition and limit carbon retention.

The impact of fertilization on soil carbon is complex and typically requires long-term observation to fully understand (Ludwig et al., 2011). Numerous studies have shown that the combined application of organic and inorganic fertilizers can contribute to SOC accumulation, whereas inappropriate fertilization practices may adversely affect various soil properties (Chen et al., 2011; Yang et al., 2015). Zhou et al. (2026) also found short-term co-application of nitrogen and organic amendments enhances MAOC. In Jiangsu Province, fertilization is dominated by nitrogen-based fertilizers. Consumption of Chemical Fertilizer exhibits a relatively negative correlation with MAOCS, which may be related to the high proportion of nitrogen fertilizers applied. This is broadly consistent with the findings of Cai and Qin (2006), who noted that although balanced application of nitrogen, phosphorus, and potassium fertilizers supports crop production, it may also be associated with reduced soil carbon sequestration under certain conditions. Furthermore, Pu et al. (2024) reported that the relationship between nitrogen fertilizer application and SOC is positively correlated over time but negatively correlated spatially. This may indicate that, spatially, higher levels of fertilization are often applied in relatively infertile areas to improve soil fertility. Such an interpretation is consistent with our findings, which show a spatially negative correlation between nitrogen-dominated fertilization and carbon stock, yet higher SOC levels in Anthrosols that have experienced long-term fertilization and cultivation.

Total Consumption of Electricity of the Year and Total Consumption of Industrial Electricity of the Year both exhibit a positive correlation with MAOCS, and a negative correlation with MAOCS deficit and carbon sequestration potential. Similarly, the number of Employed Persons for Secondary Industry shows the same trend. Since this study focuses specifically on cropland areas, industrial land is not within the scope of analysis. Therefore, it is not appropriate to directly infer a causal relationship between industrial development and soil carbon dynamics. Instead, one possible explanation is that, during economic development and urbanization, the transition from primary to secondary and tertiary industries may be associated with constraints on regional agricultural expansion. This reduction in land reclamation and cultivation activities may be associated with lower levels of soil carbon depletion, thereby resulting in lower carbon sequestration potential. In Jiangsu Province, cities with relatively well-developed industries are primarily located in the southern Yangtze River region. The rapid development of industry began after China's Reform and Opening-up in 1978 (http://www.jiangsu.gov.cn/art/2024/10/3/art_91230_11377248.html), which is relatively recent compared to the long-term influence of agricultural activities on soil carbon. Moreover, existing literature suggests that the development of industrial parks and related industrial expansion can also be associated with the loss of surface soil organic carbon (Kim et al., 2025). Therefore, the influence of industrial development in Jiangsu—such as an increase in Employed Persons for Secondary Industry and a decline in Employed Persons for Primary Industry—on soil carbon stock requires further investigation and discussion.

5.3. Implications, limitation, and future perspectives

In recent years, the estimation of carbon sequestration potential has shown a shift from traditional experimental stations and field trials toward broader regional-scale studies, including national and global assessments. (Georgiou et al., 2022; Lessmann et al., 2022; Qin et al., 2013). In our study, we conducted statistical analyses at finer administrative scales using 90 m resolution grids, aiming to achieve more detailed and precise results. Compared with traditional approaches based on total organic carbon (TOC) or bulk SOC measurements, this study focused on MAOC because it represents the mineral-associated and more persistent fraction of soil organic carbon. Bulk SOC contains substantial labile carbon pools with relatively rapid turnover, which may overestimate the stability of stored carbon. In contrast, MAOC is protected through interactions with mineral surfaces and generally exhibits longer residence times, making it more closely linked to long-term carbon stabilization and sequestration capacity (Georgiou et al., 2022; Kleber et al., 2021; Lavallee et al., 2020). Therefore, MAOC serves as a more robust indicator for evaluating the long-term potential of soil carbon storage.

In addition, whereas previous studies mainly emphasized the effects of climate, soil properties, and topographic factors on soil carbon storage, this study explicitly linked human activity indicators with MAOC deficits and carbon sequestration potential. By integrating anthropogenic factors into the analysis, the study provided a more comprehensive understanding of the spatial variability in soil carbon stabilization capacity and the potential influence of human activities on long-term carbon sequestration.

To ensure the sustainable development of agriculture, practices such as crop rotation, intercropping, or cover cropping can be further introduced, in combination with straw return and reduced soil disturbance, to mitigate the excessive depletion of soil carbon. In addition to enhancing agricultural sustainability, protecting soil carbon and increasing its sequestration contributes to expanding carbon sinks, mitigating climate change, and restoring soil biodiversity. These efforts, in turn, help to strengthen ecosystem resilience and support the achievement of global biodiversity goals.

This study estimated the carbon sequestration potential of cropland in Jiangsu Province based on the MAOC concentration of soil samples using a frontier line approach, and further integrated spatial Quantile Random Forest predictions to characterize its spatial distribution at the provincial scale. In addition, human activity indicators were incorporated to explore their potential associations with spatial variability in carbon sequestration potential, thereby providing a more comprehensive framework that combines upper-bound estimation, spatial prediction, and anthropogenic context, quantifying carbon potential and its relationship with human activities.

However, since the soil sample data were limited to a single year, the study cannot fully capture the temporal dynamics of how human activities affect soil carbon and carbon sequestration potential. In particular, the use of human activity indicators from one year may not fully represent long-term or interannual variations in anthropogenic influences on soil carbon processes. Therefore, the relationships observed in this study should be interpreted as reflecting mainly short-term spatial associations. In addition, human activity indicators were analyzed at the city or county level, which, to some extent, limits the spatial resolution of the analysis.

Although the number of soil samples (84 samples) was relatively limited for province-scale mapping, the conditioned Latin hypercube sampling (cLHS) strategy helped reduce sampling bias. However, limited sample density and randomness of cLHS may still introduce uncertainty when extrapolating model predictions to environmentally heterogeneous or sparsely represented areas (Yang et al., 2020), which could influence the accuracy of provincial-scale estimates of MAOC sequestration potential. Future study could use more samples or other sampling methods to further enhance representativeness (Yang et al., 2013). In addition, although QRF is generally considered robust to overfitting due to its ensemble structure, it can still exhibit overfitting, particularly when trees are grown deeply or when the sample size is limited. Since the estimates of MAOCS deficit and carbon sequestration potential were derived from QRF predictions, uncertainties in the QRF model may propagate into subsequent calculations and affect the reliability of the estimated sequestration potential. That occurs because QRF prediction errors are transferred directly into derived variables through arithmetic operations, and such errors may be further amplified when multiple derived indicators are computed sequentially. In addition, as carbon sequestration potential is calculated based on MAOCS deficit, uncertainties in the initial QRF predictions may accumulate through this chain of derivations, potentially influencing both the magnitude and spatial distribution of the final estimates (Barreñada et al., 2024; Fox et al., 2017; Szatmári and Pásztor, 2019; Vaysse and Lagacherie, 2017).

As for the frontier line, the estimated boundary may be influenced by measurement errors or extreme values, and this method hardly distinguish random noise from true inefficiency, which also potentially biasing the results (McKenzie, 2018). In practical applications, the frontier line approach may perform differently under varying environmental and management conditions, particularly in heterogeneous landscapes where soil properties and management practices vary substantially across space. Under such conditions, the estimated frontier may be sensitive to data sparsity and uneven sampling across environmental gradients, which may affect the robustness of the inferred boundary. Therefore, while the frontier line approach provides a useful tool for estimating potential upper limits of MAOC, its interpretation should consider underlying environmental variability and management heterogeneity, and the results should be treated with caution when extrapolating across regions with differing conditions.

Future research could benefit from multi-year soil samples to enable temporal analyses of long-term human impacts, tracking year-to-year changes in human activity intensity would help assess the sensitivity of soil carbon and sequestration potential to such changes. Future research could also explore the impact of different crop types on soil carbon sequestration potential, further providing insights for crop selection and management strategies. In addition, incorporating uncertainty quantification approaches could help further constrain these uncertainties. Meanwhile, the study area could be expanded to include forests, wetlands, and other ecosystems, incorporating natural environmental covariates for a more comprehensive analysis.

6. Conclusion

This study integrated a frontier line approach and quantile random forest to assess the spatial distribution of MAOCS deficit and carbon sequestration potential of cropland area in Jiangsu Province, explored the influences from human activities in soil orders and administrative units. The results indicate that carbon sequestration potential across Jiangsu is influenced by a combination of soil type, topography, climate conditions, and the intensity of human activities. The central-western regions and areas surrounding lakes exhibit higher carbon sequestration potential, whereas regions with higher levels of urbanization tend to show lower carbon sequestration potential. This study improves the understanding of the spatial patterns of carbon sequestration potential in agricultural areas through spatially explicit analysis, and provides a scientific basis for developing location-specific strategies to promote sustainable agricultural development. In the future, optimizing tillage practices, promoting the substitution of chemical fertilizers with organic alternatives, and advancing conservation tillage could enhance soil organic carbon stability. These strategies will provide strong support for regional sustainable agricultural development and climate change mitigation.

CRediT authorship contribution statement

Wenkai Cui: Writing – review & editing, Writing – original draft, Visualization, Validation, Supervision, Software, Resources, Project administration, Methodology, Investigation, Formal analysis, Data curation, Conceptualization. **Jie Liu:** Writing – review & editing, Resources, Data curation. **Lei Zhang:** Writing – review & editing, Supervision, Software. **Chenconghai Yang:** Writing – review & editing, Visualization, Validation. **Feixue Shen:** Writing – review & editing, Project administration, Investigation. **Lin Yang:** Writing – review & editing, Supervision, Resources, Funding acquisition, Conceptualization.

Declaration of competing interest

The authors declare that they have no known competing financial interests or personal relationships that could have appeared to influence the work reported in this paper.

Acknowledgements

This study was supported by the National Natural Science Foundation of China (Grant No. 42471468); the Postgraduate Research & Practice Innovation Program of Jiangsu Province (Grant No. KYCX25_0209).

Appendix A. Supplementary data

Supplementary data to this article can be found online at https://doi.org/10.1016/j.catena.2026.110383.

Data availability

Reference data (Reference data) (Figshare)

References

Amelung, W., Bossio, D., de Vries, W., Kögel-Knabner, I., Lehmann, J., Amundson, R., Bol, R., Collins, C., Lal, R., Leifeld, J., Minasny, B., Pan, G., Paustian, K., Rumpel, C., Sanderman, J., van Groenigen, J.W., Mooney, S., van Wesemael, B., Wander, M., Chabbi, A., 2020. Towards a global-scale soil climate mitigation strategy. Nat. Commun. 11, 5427. https://doi.org/10.1038/s41467-020-18887-7.

Arias, P., Bellouin, N., Coppola, E., Jones, R., Krinner, G., Marotzke, J., Naik, V., Palmer, M., Plattner, G.-K., Rogelj, J., Rojas, M., Sillmann, J., Storelvmo, T., Thorne, P., Trewin, B., Achutarao, K., Adhikary, B., Allan, R., Armour, K., Bala, G., Barimalala, R., Berger, S., Canadell, J.G., Cassou, C., Cherchi, A., Collins, W.D., Collins, W.J., Connors, S., Corti, S., Cruz, F., Dentener, F.J., Dereczynski, C., Di Luca, A., Diongue Niang, A., Doblas-Reyes, P., Dosio, A., Douville, H., Engelbrecht, F., Eyring, V., Fischer, E.M., Forster, P., Fox-Kemper, B., Fuglestvedt, J., Fyfe, J., Gillett, N., Goldfarb, L., Gorodetskaya, I., Gutierrez, J.M., Hamdi, R., Hawkins, E., Hewitt, H., Hope, P., Islam, A.S., Jones, C., Kaufmann, D., Kopp, R., Kosaka, Y., Kossin, J., Krakovska, S., Li, J., Lee, J.-Y., Masson-Delmotte, V., Mauritsen, T., Maycock, T., Meinshausen, M., Min, S., Ngo Duc, T., Otto, F., Pinto, I., Pirani, A., Raghavan, K., Ranasighe, R., Ruane, A., Ruiz, L., Sallée, J.-B., Samset, B. H., Sathyendranath, S., Monteiro, P.S., Seneviratne, S.I., Sörensson, A.A., Szopa, S., Takayabu, I., Treguier, A.-M., van den Hurk, B., Vautard, R., Von Schuckmann, K., Zaehle, S., Zhang, X., Zickfeld, K., 2021. Climate change 2021: the physical science basis. Contribution of working group I to the sixth assessment report of the

intergovernmental panel on climate change; technical summary [WWW document]. URL. https://www.ipcc.ch/report/ar6/wg1/.
Barreñada, L., Dhiman, P., Timmerman, D., Boulesteix, A.-L., Van Calster, B., 2024. Understanding overfitting in random forest for probability estimation: a visualization and simulation study. Diagn. Progn. Res. 8, 14. https://doi.org/10.1186/s41512-024-00177-1.
Batjes, N.H., 2014. Total carbon and nitrogen in the soils of the world. Eur. J. Soil Sci. 65, 10–21. https://doi.org/10.1111/ejss.12114_2.
Beare, M.H., McNeill, S.J., Curtin, D., Parfitt, R.L., Jones, H.S., Dodd, M.B., Sharp, J., 2014. Estimating the organic carbon stabilisation capacity and saturation deficit of soils: a New Zealand case study. Biogeochemistry 120, 71–87. https://doi.org/10.1007/s10533-014-9982-1.
Bogaert, P., Taghizadeh-Mehrjardi, R., Hamzehpour, N., 2023. Model averaging of machine learning algorithms for digital soil mapping: a minimum variance framework. Geoderma 437, 116604. https://doi.org/10.1016/j.geoderma.2023.116604.
Bossio, D.A., Cook-Patton, S.C., Ellis, P.W., Fargione, J., Sanderman, J., Smith, P., Wood, S., Zomer, R.J., von Unger, M., Emmer, I.M., Griscom, B.W., 2020. The role of soil carbon in natural climate solutions. Nat. Sustain. 3, 391–398. https://doi.org/10.1038/s41893-020-0491-z.
Breure, T.S., De Rosa, D., Panagos, P., Cotrufo, M.F., Jones, A., Lugato, E., 2025. Revisiting the soil carbon saturation concept to inform a risk index in European agricultural soils. Nat. Commun. 16, 2538. https://doi.org/10.1038/s41467-025-57355-y.
Cai, Z.C., Qin, S.W., 2006. Dynamics of crop yields and soil organic carbon in a long-term fertilization experiment in the Huang-Huai-Hai plain of China. Geoderma 136, 708–715. https://doi.org/10.1016/j.geoderma.2006.05.008.
Chen, S., Arrouays, D., Angers, D.A., Chenu, C., Barré, P., Martin, M.P., Saby, N.P.A., Walter, C., 2019. National estimation of soil organic carbon storage potential for arable soils: a data-driven approach coupled with carbon-landscape zones. Sci. Total Environ. 666, 355–367. https://doi.org/10.1016/j.scitotenv.2019.02.249.
Chen, X., Swanson, N.R. (Eds.), 2013. Recent Advances and Future Directions in Causality, Prediction, and Specification Analysis: Essays in Honor of Halbert L. White Jr.. Springer New York, New York, NY. https://doi.org/10.1007/978-1-4614-1653-1.
Chen, X., Zhang, L.-M., Shen, J.-P., Wei, W.-X., He, J.-Z., 2011. Abundance and community structure of ammonia-oxidizing archaea and bacteria in an acid paddy soil. Biol. Fertil. Soils 47, 323–331. https://doi.org/10.1007/s00374-011-0542-8.
Cotrufo, M.F., 2019. Soil carbon storage informed by particulate and mineral-associated organic matter. Nat. Geosci. 12.
Cui, X., Cai, T., Deng, W., Zheng, R., Jiang, Y., Bao, H., 2022. Indicators for evaluating high-quality agricultural development: empirical study from Yangtze River Economic Belt. China. Soc. Indic. Res. 164, 1101–1127. https://doi.org/10.1007/s11205-022-02985-8.
De Rosa, D., Ballabio, C., Lugato, E., Fasiolo, M., Jones, A., Panagos, P., 2024. Soil organic carbon stocks in European croplands and grasslands: how much have we lost in the past decade? Glob. Change Biol. 30, e16992. https://doi.org/10.1111/gcb.16992.
Dendooven, L., Alcántara-Hernández, R.J., Valenzuela-Encinas, C., Luna-Guido, M., Perez-Guevara, F., Marsch, R., 2010. Dynamics of carbon and nitrogen in an extreme alkaline saline soil: a review. Soil Biol. Biochem. 42, 865–877. https://doi.org/10.1016/j.soilbio.2010.02.014.
Du, Y., Xue, H., Wu, S., Ling, F., Xiao, F., Wei, X., 2011. Lake area changes in the middle Yangtze region of China over the 20th century. J. Environ. Manage. 92, 1248–1255. https://doi.org/10.1016/j.jenvman.2010.12.007.
Feng, W., Plante, A.F., Six, J., 2013. Improving estimates of maximal organic carbon stabilization by fine soil particles. Biogeochemistry 112, 81–93. https://doi.org/10.1007/s10533-011-9679-7.
Fox, E.W., Hill, R.A., Leibowitz, S.G., Olsen, A.R., Thornbrugh, D.J., Weber, M.H., 2017. Assessing the accuracy and stability of variable selection methods for random forest modeling in ecology. Environ. Monit. Assess. 189, 316. https://doi.org/10.1007/s10661-017-6025-0.
Georgiou, K., Jackson, R.B., Vindušková, O., Abramoff, R.Z., Ahlström, A., Feng, W., Harden, J.W., Pellegrini, A.F.A., Polley, H.W., Soong, J.L., Riley, W.J., Torn, M.S., 2022. Global stocks and capacity of mineral-associated soil organic carbon. Nat. Commun. 13, 3797. https://doi.org/10.1038/s41467-022-31540-9.
Ghollarata, M., Raiesi, F., 2007. The adverse effects of soil salinization on the growth of Trifolium alexandrinum L. and associated microbial and biochemical properties in a soil from Iran. Soil Biol. Biochem. 39, 1699–1702. https://doi.org/10.1016/j.soilbio.2007.01.024.
Gregorich, E.G., Carter, M.R., Angers, D.A., Drury, C.F., 2009. Using a sequential density and particle-size fractionation to evaluate carbon and nitrogen storage in the profile of tilled and no-till soils in eastern Canada. Can. J. Soil Sci. 89, 255–267. https://doi.org/10.4141/CJSS08034.
Hassink, J., 1997. The capacity of soils to preserve organic C and N by their association with clay and silt particles. Plant and Soil 191, 77–87. https://doi.org/10.1023/A:1004213929699.
Hassink, J., Whitmore, A.P., 1997. A model of the physical protection of organic matter in soils. Soil Sci. Soc. Am. J. 61, 131–139. https://doi.org/10.2136/sssaj1997.03615995006100010020x.
Holliday, V.T., 2022. Anthrosols, in: Gilbert, A.S., Goldberg, P., Mandel, R.D., Aldeias, V. (Eds.), Encyclopedia of Geoarchaeology, Encyclopedia of Earth Sciences Series. Springer International Publishing, Cham, pp. 1–4. Doi: https://doi.org/10.1007/978-3-030-44600-0_130-1.
Ju, J., Zhao, L., Wang, J., 2016. Fluctuations influence factors analysis of growth of agricultural machinery total power. Trans. Chin. Soc. Agric. Eng. 32, 84–91.
Khaledian, Y., Miller, B.A., 2020. Selecting appropriate machine learning methods for digital soil mapping. App. Math. Model. 81, 401–418. https://doi.org/10.1016/j.apm.2019.12.016.
Kim, Y.I., Jang, W.S., Shin, K.-H., Oh, S.J., Engel, B., Doro, L., 2025. Estimation of potential topsoil organic carbon loss due to industrial complex development: implications for topsoil conservation in South Korea. Environ. Impact Assess. Rev. 111, 107739. https://doi.org/10.1016/j.eiar.2024.107739.
Kleber, M., Bourg, I.C., Coward, E.K., Hansel, C.M., Myneni, S.C.B., Nunan, N., 2021. Dynamic interactions at the mineral–organic matter interface. Nat. Rev. Earth Environ. 2, 402–421. https://doi.org/10.1038/s43017-021-00162-y.
Kuhn, M., 2007. caret: Classification and Regression Training. https://doi.org/10.32614/CRAN.package.caret.
Kuhn, M., 2008. Building predictive models in *R* using the **caret** package. J. Stat. Softw. 28. https://doi.org/10.18637/jss.v028.i05.
Lal, R., 2004a. Soil carbon sequestration impacts on global climate change and food security. Science 304, 1623–1627. https://doi.org/10.1126/science.1097396.
Lal, R., 2004b. Agricultural activities and the global carbon cycle. Nutr. Cycl. Agroecosystems 70, 103–116. https://doi.org/10.1023/B:FRES.0000048480.24274.0f.
Lavallee, J.M., Soong, J.L., Cotrufo, M.F., 2020. Conceptualizing soil organic matter into particulate and mineral-associated forms to address global change in the 21st century. Glob. Change Biol. 26, 261–273. https://doi.org/10.1111/gcb.14859.
Lessmann, M., Ros, G.H., Young, M.D., De Vries, W., 2022. Global variation in soil carbon sequestration potential through improved cropland management. Glob. Change Biol. 28, 1162–1177. https://doi.org/10.1111/gcb.15954.
Likhanova, I.A., Deneva, S.V., Kholopov, Y.V., Kuznetsova, E.G., Shakhtarova, O.V., Lapteva, E.M., 2022. The effect of Hydromorphism on soils and soil organic matter during the primary succession processes of Forest vegetation on ancient Alluvial Sands of the European north-east of Russia. Forests 13, 230. https://doi.org/10.3390/f13020230.
Lu, F., 2015. How can straw incorporation management impact on soil carbon storage? A meta-analysis. Mitig. Adapt. Strateg. Glob. Change 20, 1545–1568. https://doi.org/10.1007/s11027-014-9564-5.
Ludwig, B., Geisseler, D., Michel, K., Joergensen, R.G., Schulz, E., Merbach, I., Raupp, J., Rauber, R., Hu, K., Niu, L., Liu, X., 2011. Effects of fertilization and soil management on crop yields and carbon stabilization in soils. A review. Agron. Sustain. Dev. 31, 361–372. https://doi.org/10.1051/agro/2010030.
Mao, C., Kou, D., Chen, L., Qin, S., Zhang, D., Peng, Y., Yang, Y., 2020. Permafrost nitrogen status and its determinants on the Tibetan plateau. Glob. Change Biol. 26, 5290–5302. https://doi.org/10.1111/gcb.15205.
Marriott, E.E., Wander, M., 2006. Qualitative and quantitative differences in particulate organic matter fractions in organic and conventional farming systems. Soil Biol. Biochem. 38, 1527–1536. https://doi.org/10.1016/j.soilbio.2005.11.009.
McKenzie, T., 2018. snfa: Smooth Non-Parametric Frontier Analysis. https://doi.org/10.32614/CRAN.package.snfa.
Meng, M., Yu, L., Yu, X., 2024. Machinery structure, machinery subsidies, and agricultural productivity: evidence from China. Agric. Econ. 55, 223–246. https://doi.org/10.1111/agec.12820.
Minasny, B., McBratney, A.B., 2006. A conditioned Latin hypercube method for sampling in the presence of ancillary information. Comput. Geosci. 32, 1378–1388. https://doi.org/10.1016/j.cageo.2005.12.009.
Nikou, M., Tziachris, P., 2022. Prediction and uncertainty capabilities of quantile regression forests in estimating spatial distribution of soil organic matter. ISPRS Int. J. Geo Inf. 11, 130. https://doi.org/10.3390/ijgi11020130.
Nolan, C.J., Field, C.B., Mach, K.J., 2021. Constraints and enablers for increasing carbon storage in the terrestrial biosphere. Nat. Rev. Earth Environ. 2, 436–446. https://doi.org/10.1038/s43017-021-00166-8.
Office for the Second National Soil Survey of China, 1993. Soil Species of China, 1. Chinese Agriculture Press, Beijing, China.
Pathak, H., Rao, D.L.N., 1998. Carbon and nitrogen mineralization from added organic matter in saline and alkali soils. Soil Biol. Biochem. 30, 695–702. https://doi.org/10.1016/S0038-0717(97)00208-3.
Peng, S., 2019. 1-Km Monthly Mean Temperature Dataset for China (1901–2023) [dataset]. National Tibetan Plateau/Third Pole Environment Data Center.
Peng, S., 2020. 1-Km Monthly Precipitation Dataset for China (1901–2020) [Dataset]. Natl. Tibet. Plateau Data Cent., Beijing China.
Peng, S., 2022. 1-Km Monthly Potential Evapotranspiration Dataset in China (1990–2021) [Dataset]. Natl. Tibet. Plateau Data Cent, Beijing China.
Pikuła, D., Pauková, Ž., Wójcik-Gront, E., Šimanský, V., 2025. The relationship between organic carbon and Ca in the profile of Luvisols: a case study of a long-term experiment in Pulawy, Poland. Agriculture 15, 598. https://doi.org/10.3390/agriculture15060598.
Poeplau, C., Don, A., 2015. Carbon sequestration in agricultural soils via cultivation of cover crops – a meta-analysis. Agric. Ecosyst. Environ. 200, 33–41. https://doi.org/10.1016/j.agee.2014.10.024.
Post, W.M., Izaurralde, R.C., Mann, L.K., Bliss, N., 2001. Monitoring and verifying changes of organic carbon in soil. In: Rosenberg, N.J., Izaurralde, Roberto C. (Eds.), Storing Carbon in Agricultural Soils: A Multi-Purpose Environmental Strategy. Springer Netherlands, Dordrecht, pp. 73–99. https://doi.org/10.1007/978-94-017-3089-1_4.
Prairie, A.M., King, A.E., Cotrufo, M.F., 2023. Restoring particulate and mineral-associated organic carbon through regenerative agriculture. Proc. Natl. Acad. Sci. 120, e2217481120. https://doi.org/10.1073/pnas.2217481120.
Pu, Y., Yang, L., Zhang, L., Huang, H., Zhang, G., Zhou, C., 2024. Major contributions of agricultural management practices to topsoil organic carbon distribution and

accumulation in croplands of East China over three decades. Agric. Ecosyst. Environ. 359, 108749. https://doi.org/10.1016/j.agee.2023.108749.
Qin, Z., Huang, Y., Zhuang, Q., 2013. Soil organic carbon sequestration potential of cropland in China. Global Biogeochem. Cycles 27, 711–722. https://doi.org/10.1002/gbc.20068.
Schlesinger, W.H., Andrews, J.A., 2000. Soil respiration and the global carbon cycle. Biogeochemistry 48, 7–20. https://doi.org/10.1023/A:1006247623877.
Shi, G., Sun, W., Shangguan, W., Wei, Z., Yuan, H., Li, L., Sun, X., Zhang, Y., Liang, H., Li, D., Huang, F., Li, Q., Dai, Y., 2025. A China dataset of soil properties for land surface modelling (version 2, CSDLv2) [dataset]. Earth Syst. Sci. Data 17, 517–543. https://doi.org/10.5194/essd-17-517-2025.
Six, J., Conant, R.T., Paul, E.A., Paustian, K., 2002. Stabilization mechanisms of soil organic matter: implications for C-saturation of soils. Plant and Soil 241, 155–176. https://doi.org/10.1023/A:1016125726789.
Six, J., Doetterl, S., Laub, M., Müller, C.R., Van De Broek, M., 2024. The six rights of how and when to test for soil C saturation. SOIL 10, 275–279. https://doi.org/10.5194/soil-10-275-2024.
Song, X., Peng, C., Zhou, G., Jiang, H., Wang, W., 2014. Chinese grain for green program led to highly increased soil organic carbon levels: a meta-analysis. Sci. Rep. 4, 4460. https://doi.org/10.1038/srep04460.
Stewart, C.E., Paustian, K., Conant, R.T., Plante, A.F., Six, J., 2007. Soil carbon saturation: concept, evidence and evaluation. Biogeochemistry 86, 19–31. https://doi.org/10.1007/s10533-007-9140-0.
Szatmári, G., Pásztor, L., 2019. Comparison of various uncertainty modelling approaches based on geostatistics and machine learning algorithms. Geoderma 337, 1329–1340. https://doi.org/10.1016/j.geoderma.2018.09.008.
Tao, F., Palosuo, T., Valkama, E., Mäkipää, R., 2019. Cropland soils in China have a large potential for carbon sequestration based on literature survey. Soil Tillage Res. 186, 70–78. https://doi.org/10.1016/j.still.2018.10.009.
Tripathi, S., Chakraborty, A., Chakrabarti, K., Bandyopadhyay, B.K., 2007. Enzyme activities and microbial biomass in coastal soils of India. Soil Biol. Biochem. 39, 2840–2848. https://doi.org/10.1016/j.soilbio.2007.05.027.
Vaysse, K., Lagacherie, P., 2017. Using quantile regression forest to estimate uncertainty of digital soil mapping products. Geoderma 291, 55–64. https://doi.org/10.1016/j.geoderma.2016.12.017.
Viscarra Rossel, R.A., Webster, R., Zhang, M., Shen, Z., Dixon, K., Wang, Y.-P., Walden, L., 2024. How much organic carbon could the soil store? The carbon sequestration potential of Australian soil. Glob. Change Biol. 30, e17053. https://doi.org/10.1111/gcb.17053.
Wang, W., Guo, Y., Yang, L., Adams, J.M., 2024. Methanogen–methanotroph community has a more consistent and integrated structure in rice rhizosphere than in bulk soil and rhizoplane. Mol. Ecol. 33, e17416. https://doi.org/10.1111/mec.17416.
Wenzel, W.W., Duboc, O., Golestanifard, A., Holzinger, C., Mayr, K., Reiter, J., Schiefer, A., 2022. Soil and land use factors control organic carbon status and accumulation in agricultural soils of Lower Austria. Geoderma 409, 115595. https://doi.org/10.1016/j.geoderma.2021.115595.
Wichern, J., Wichern, F., Joergensen, R.G., 2006. Impact of salinity on soil microbial communities and the decomposition of maize in acidic soils. Geoderma 137, 100–108. https://doi.org/10.1016/j.geoderma.2006.08.001.
Wiesmeier, M., Hübner, R., Spörlein, P., Geuß, U., Hangen, E., Reischl, A., Schilling, B., Von Lützow, M., Kögel-Knabner, I., 2014. Carbon sequestration potential of soils in Southeast Germany derived from stable soil organic carbon saturation. Glob. Change Biol. 20, 653–665. https://doi.org/10.1111/gcb.12384.
Wong, V.N.L., Greene, R.S.B., Dalal, R.C., Murphy, B.W., 2010. Soil carbon dynamics in saline and sodic soils: a review: soil carbon dynamics in saline and sodic soils. Soil Use Manage. 26, 2–11. https://doi.org/10.1111/j.1475-2743.2009.00251.x.
Woolf, D., Lehmann, J., 2019. Microbial models with minimal mineral protection can explain long-term soil organic carbon persistence. Sci. Rep. 9, 6522. https://doi.org/10.1038/s41598-019-43026-8.
Xu, S., Liu, X., Li, X., Tian, C., 2019. Soil organic carbon changes following wetland restoration: a global meta-analysis. Geoderma 353, 89–96. https://doi.org/10.1016/j.geoderma.2019.06.027.
Yang, J., Huang, X., 2023. The 30 m annual land cover datasets and its dynamics in China from 1985 to 2022 [dataset]. Doi: https://doi.org/10.5281/ZENODO.8176941.
Yang, J., Gao, W., Ren, S., 2015. Long-term effects of combined application of chemical nitrogen with organic materials on crop yields, soil organic carbon and total nitrogen in fluvo-aquic soil. Soil Tillage Res. 151, 67–74. https://doi.org/10.1016/j.still.2015.03.008.
Yang, L., Zhu, A.-X., Qi, F., Qin, C.-Z., Li, B., Pei, T., 2013. An integrative hierarchical stepwise sampling strategy for spatial sampling and its application in digital soil mapping. Int. J. Geogr. Inf. Sci. 27, 1–23. https://doi.org/10.1080/13658816.2012.658053.
Yang, L., Li, X., Shi, J., Shen, F., Qi, F., Gao, B., Chen, Z., Zhu, A.-X., Zhou, C., 2020. Evaluation of conditioned Latin hypercube sampling for soil mapping based on a machine learning method. Geoderma 369, 114337. https://doi.org/10.1016/j.geoderma.2020.114337.
Yang, L., Shen, F., Zhang, L., Cai, Y., Yi, F., Zhou, C., 2021. Quantifying influences of natural and anthropogenic factors on vegetation changes using structural equation modeling: a case study in Jiangsu Province, China. J. Clean. Prod. 280, 124330. https://doi.org/10.1016/j.jclepro.2020.124330.
Yin, S., Yi, Y., Liu, Q., Luo, Q., Chen, K., 2022. A review on effects of human activities on aquatic organisms in the Yangtze River basin since the 1950s. River 1, 104–119. https://doi.org/10.1002/rvr2.15.
Zhang, C., Yang, L., Wiedenhofer, D., Guo, J., Chen, Z., Li, S., Wang, Z., Kwan, M., Zhou, Y., Lin, L., Zhang, L., Li, M., Zhu, Q., Yu, B., Chen, B., Yan, X., Wang, X., Gao, B., Liang, Y., Hu, J., Fu, Y., Lv, Q., Yang, J., Wang, Y., Wang, Qianqian, Wang, Qiao, 2026. Building material stock drives embodied carbon emissions and risks future climate goals in China. Nat. Clim. Chang. 16, 164–171. https://doi.org/10.1038/s41558-025-02527-3.
Zhou, R., Xue, Y., Kumar, A., Gunina, A., Ling, J., Cui, Z., Kuzyakov, Y., Tian, J., 2026. Particulate and mineral-associated organic matter in cropland soils: Meta-analysis of management effects. Agric. Ecosyst. Environ. 400, 110218. https://doi.org/10.1016/j.agee.2026.110218.
Zomer, R.J., Bossio, D.A., Sommer, R., Verchot, L.V., 2017. Global sequestration potential of increased organic carbon in cropland soils. Sci. Rep. 7, 15554. https://doi.org/10.1038/s41598-017-15794-8.